Fractionalized Fermi liquid on the surface of a topological Kondo insulator

Alex Thomson and Subir Sachdev

Phys. Rev. B **93**, 125103 — Published 1 March 2016

DOI: 10.1103/PhysRevB.93.125103

Fractionalized Fermi liquid on the surface of a topological Kondo insulator

Alex Thomson[1] and Subir Sachdev[1,2]

[1] *Department of Physics, Harvard University, Cambridge, Massachusetts, 02138, USA*

[2] *Perimeter Institute for Theoretical Physics, Waterloo, Ontario N2L 2Y5, Canada*

(Dated: February 3, 2016)

Abstract

We argue that topological Kondo insulators can also have 'intrinsic' topological order associated with fractionalized excitations on their surfaces. The hydridization between the local moments and conduction electrons can weaken near the surface, and this enables the local moments to form spin liquids. This co-exists with the conduction electron surface states, realizing a surface fractionalized Fermi liquid. We present mean-field solutions of a Kondo-Heisenberg model in two spatial dimensions which display such surfaces.

I. INTRODUCTION

An important development of the past decade has been the prediction and discovery of topological insulators (TI) [1–7]. These materials are well-described by traditional band theory, but possess strong spin-orbit interactions that result in a non-trivial winding of the ground state wavefunction in a manner analogous to the integer quantum Hall effect. Since their discovery, the multitudinous effects of interactions have been a prominent topic of study. One compelling proposal to emerge is the notion of a topological *Kondo* insulator (TKI) [8–10]. In contrast to a band insulator, a Kondo insulator only develops an insulating gap at low temperatures, and the magnitude of the gap is controlled by electron-electron interactions. Doniach explained this phenomenon through the Kondo lattice model [11] in which a lattice of localized moments is immersed within a sea of conduction electrons. When the spin exchange is weak, RKKY-type interactions dominate and an ordered magnetic state results. Conversely, strong interactions between localized moments and conduction electrons push the system into a metallic phase well-described by Fermi liquid theory (FL) or, if the chemical potential is appropriately tuned, a Kondo insulator. As strong spin-orbit coupling is often present in these materials, the possibility that a Kondo insulator may have a nontrivial topological character is well-justified.

Of specific interest has been the Kondo insulator samarium hexaboride (SmB_6). A number of experiments have examined the proposal that it is a TKI: transport measurements have established the presence of metallic surface states [12–16], and angle-resolved photoemission spectroscopy (ARPES) results appear consistent with the expected Dirac surface cones [17–21]. Nonetheless, the spin-polarized ARPES measurements [21] remain controversial.

However, as the TKI phase is well-described within a mean field framework [10], its topological properties are not expected to be markedly different from what has already been observed in its uncorrelated cousins. More intriguing is the potential the topologically protected surface states present for new interesting phases [22–25]. In SmB_6, this expectation is motivated experimentally by ARPES measurements which find light surface quasiparticles [17–19] in contradiction to current theories which predict heavy particles at the surface [8, 9, 26, 27]. Ref. [24] proposes "Kondo breakdown" at the surface as an explanation. They show that the reduced coordination number of the localized moments at the surface may lead to a suppressed Kondo temperature. At low temperature these moments are thermally decoupled from the bulk.

In this paper, we propose the existence of a fractionalized Fermi liquid (SFL*) on the surface of a TKI. This state is characterized by "*intrinsic* topological order" on the surface of a TKI, in which the local moments form a spin liquid state which has 'fractionalized' excitations with quantum numbers which cannot be obtained by combining those of one or more electrons [28]. Rather than being thermally liberated, as in Ref. 24, the surface local moments exploit their mutual exchange interactions to decouple from the conduction electrons, and form a spin liquid state, as in the fractionalized Fermi liquid state (FL*) [29, 30]. We will present mean-field computations on a Kondo-Heisenberg lattice model which demonstrate the formation of mutual singlets between the surface local moments, while conducting surface states of light electronic quasiparticles are also present. For numerical simplicity, we will be working in two spatial dimensions.

Somewhat confusingly, our SFL* state is 'topological' in two senses of the word, a consequence of unfortunate choices (from our perspective) in the conventional terminology. As in conventional TI, it is 'topological' because it has gapless electronic states on the surface induced by the nature of the bulk band structure. However, it is also 'topological' in the sense of spin liquids [28], because of the presence of fractionalized excitations among the local moments on the surface.

The outline of our paper is as follows. We specify our Kondo-Heisenberg model in Section II. In Section III, we present the mean-field solution of this model for the case of a translationally-invariant square lattice with periodic boundary conditions. The effect of the surface on the mean field solutions is addressed in Section IV where the presence of the SFL* state is numerically demonstrated. We conclude in Section V with a discussion of our results and their relevance to physical systems.

II. MODEL

Here we present the specific form of the Kondo-Heisenberg lattice model to be studied:

$$H = H_c + H_H + H_K \, . \tag{1}$$

The first terms represents the hopping Hamiltonian of the conduction electrons,

$$H_c = -\sum_{\langle ij \rangle} t_{ij} \left(c^\dagger_{i\alpha} c_{j\alpha} + h.c. \right) \, , \tag{2}$$

where the operator $c^\dagger_{i\alpha}$ creates an electron at site $\mathbf{r}_i$ of spin $\alpha =\uparrow,\downarrow$. The remaining two terms establish the form of the interactions: H_K is a Kondo term and describes the electron-spin exchange while H_H is a generalized Heisenberg term which specifies the inter-spin interaction.

For the electron-spin interaction, H_K, we follow the construction of Coqblin-Schrieffer [31] for systems with spin-orbit coupling. The spin-orbit coupling of the f-orbital imposes a classification in terms of a $(2J+1)$ multiplet, where J is the total angular momentum. In general, this degeneracy is further lifted by crystal fields and we will consider the simplest case of a Kramers degenerate pair of states. In order for the interaction to transform as a singlet, the electron and spin must couple in a higher angular momentum channel. For simplicity, we assume a square lattice with spins and conduction electrons that carry total angular momentum differing by $l = 1$. In the Anderson lattice model [32], an appropriate interaction term is then

$$H_{Alm} \sim \mathcal{V} \sum_{\mathbf{k},\alpha} (\alpha \sin k_x - i \sin k_y)\, c^\dagger_{\mathbf{k}\alpha}\, |f^0\rangle \langle f^1; \alpha| + h.c. \tag{3}$$

For instance, the interaction between moments with total angular momentum $J = 3/2$ and spin-1/2 electrons would take this form and we will verify in the next section that for the purpose of obtaining a TKI, this coupling is sufficient. The Anderson model is further supplemented by a Hubbard interaction term on the f-orbital. Since we are are specifically interested in the limit where f-orbital charge fluctuations are completely disallowed, we take the Hubbard interaction strength U_f to infinity and implement a Schrieffer-Wolff transformation [33] to obtain the Kondo term

$$H_K = -\frac{J_K}{4} \sum_i f^\dagger_{i\alpha} d_{i\alpha} d^\dagger_{i\beta} f_{i\beta}\,, \tag{4}$$

where $J_K \sim \mathcal{V}^2/U_f$. The operator $f_{i\alpha}$ annihilates a spinon at site $\mathbf{r}_i$ and $d_{i\alpha}$ is an electron operator given by

$$d_{\mathbf{k}\alpha} = 2\,(\alpha \sin k_x + i \sin k_y)\, c_{\mathbf{k}\alpha}, \qquad d_{i\alpha} = -i\alpha(c_{i+\hat{\mathbf{x}},\alpha} - c_{i-\hat{\mathbf{x}},\alpha}) + (c_{i+\hat{\mathbf{y}},\alpha} - c_{i-\hat{\mathbf{y}},\alpha})\,. \tag{5}$$

Importantly, this limit imposes the constraint $\sum_\alpha f^\dagger_{i\alpha} f_{i\alpha} = 1$ and implies that the spinon operators $f_{j\alpha}$ do not have a uniquely defined phase. In fact, by choosing to represent the spins in terms of

constrained fermion operators, we are formulating the Kondo lattice model as a U(1) gauge theory. This emergent gauge structure is what permits a realization of the fractionalized phases we will discuss [29, 30].

The Kondo term H_K will further induce an interaction between the moments, which generically will be of the form

$$H_H = \frac{J_H}{4} \sum_{\langle ij \rangle} f^\dagger_{i\alpha} \boldsymbol{\sigma}_{\alpha\beta} f_{i\beta} \cdot f^\dagger_{j\gamma} \boldsymbol{\sigma}_{\gamma\delta} f_{j\delta} = J_H \sum_{\langle ij \rangle} \mathbf{S}_i \cdot \mathbf{S}_j \,, \tag{6}$$

where the correct commutation relations for the "spin" operators $S^a_j = \frac{1}{2} f^\dagger_{j\alpha} \sigma^a_{\alpha\beta} f_{j\beta}$ are ensured by the $\sum_\alpha f^\dagger_{i\alpha} f_{i\alpha} = 1$ constraint. With the Fierz identity (and dropping a constant), we can put this in the form

$$H_H = -\frac{J_H}{2} \sum_{\langle ij \rangle} f^\dagger_{i\alpha} f_{j\alpha} f^\dagger_{j\beta} f_{i\beta} \,. \tag{7}$$

We next perform a Hubbard-Stratonovich transformation of the Kondo and Heisenberg terms:

$$\begin{aligned} H' =& H_1 + H_0 \\ H_1 =& -\sum_{\langle ij \rangle} \Big((t_{ij} - \delta_{ij}\mu_i) c^\dagger_{i\alpha} c_{j\alpha} + h.c. \Big) + \frac{1}{2} \sum_{j\alpha} \Big[V_j f^\dagger_{j\alpha} d_{j\alpha} + V^*_j d^\dagger_{j\alpha} f_{j\alpha} \Big] \\ & - \frac{1}{2} \sum_{j\alpha\hat{\boldsymbol{\mu}}} \Big[\chi_{j\mu} f^\dagger_{j+\hat{\boldsymbol{\mu}},\alpha} f_{j\alpha} + \chi^*_{j\mu} f^\dagger_{j\alpha} f_{j+\hat{\boldsymbol{\mu}},\alpha} \Big] + \sum_j \lambda_j f^\dagger_{j\alpha} f_{j\alpha} \\ H_0 =& \sum_j \left[-\lambda_j + \frac{|V_j|^2}{J_K} + \sum_{\hat{\boldsymbol{\mu}}} \frac{|\chi_{j\mu}|^2}{2J_H} \right] . \end{aligned} \tag{8}$$

We proceed with a saddle-point approximation, and treat the fields V_j, $\chi_{j\mu}$, and λ_j as real constants subject to the self-consistency conditions

$$V_j = -\frac{J_K}{2} \left\langle d^\dagger_{j\alpha} f_{j\alpha} \right\rangle , \qquad \chi_{j\mu} = J_H \left\langle f^\dagger_{j\alpha} f_{j+\hat{\boldsymbol{\mu}},\alpha} \right\rangle , \tag{9}$$

$$1 = \left\langle f^\dagger_{j\alpha} f_{j\alpha} \right\rangle . \tag{10}$$

This can be formally justified within a large-N expansion of Eq. 1, with N the number of spinons. As we are specifying to the case of an insulator, it further makes sense to require perfect half-filling.

Since $n_f = 1$ already, this results in a final equation for the chemical potential μ_j:

$$1 = \left\langle c^\dagger_{j\alpha} c_{j\alpha} \right\rangle . \tag{11}$$

III. TRANSLATIONALLY INVARIANT SYSTEM

We begin by solving Eqs. $9-11$ in a translationally invariant system with periodic boundary conditions on a square lattice. Letting $V_j = V$, $\chi_{jx} = \chi_{jy} = \chi$, $\lambda_j = \lambda$ and $\mu_j = \mu$, we perform a Fourier transform:

$$H_1 = \sum_{\mathbf{k}} \Psi^\dagger_{\mathbf{k}} \mathcal{H}(\mathbf{k}) \Psi_{\mathbf{k}} \qquad \Psi^\dagger_{\mathbf{k}} = \left(c^\dagger_{\mathbf{k}\uparrow}, f^\dagger_{\mathbf{k}\uparrow}, c^\dagger_{\mathbf{k}\downarrow}, f^\dagger_{\mathbf{k}\downarrow} \right) \tag{12}$$

$$\mathcal{H}(\mathbf{k}) = \begin{pmatrix} h(\mathbf{k}) & 0 \\ 0 & h^*(-\mathbf{k}) \end{pmatrix} \qquad h(\mathbf{k}) = \begin{pmatrix} \epsilon_c(\mathbf{k}) & V(\sin k_x + i \sin k_y) \\ V(\sin k_x - i \sin k_y) & \epsilon_f(\mathbf{k}) \end{pmatrix} . \tag{13}$$

For simplicity, we only consider nearest-neighbour coupling between spins; for the electron dispersion, a slightly more general description is required and we also take next-nearest neighbour hopping into account. The dispersions are given by

$$\epsilon_c(\mathbf{k}) = -t_1(\cos k_x + \cos k_y) - 2t_2 \cos k_x \cos k_y - \mu, \qquad \epsilon_f(\mathbf{k}) = -\chi(\cos k_x + \cos k_y) + \lambda \tag{14}$$

where the subscripts "c" and "f" refer to the electrons and spinons respectively. In the following, we will use units of energy where $t_1 = 1.0$.

Since TI's exist as a result of a band inversion, it's important to ask which sign χ will take. Naturally, when $V = 0$, the particle-hole symmetry of our mean field *ansatz* implies that $\chi > 0$ and $\chi < 0$ have the same energy. At finite hybridization, however, one will become preferable. We note that when χ and t_1 have opposite signs, the energy of the lower band will be less than the Fermi energy and hence occupied throughout most of the Brillouin zone (BZ): an increase in V will push most of these states to lower energies. Conversely, if χ and t_1 take the same sign, in one of part of the BZ no states will lie below the Fermi energy while in another both the upper and lower band will. It therefore makes sense to expect $\text{sign}\,(\chi) = -\text{sign}\,(t_1)$. In the parameter regime explored, the numerics always find this to be the case.

By construction, the Hamiltonian H_1 supports a non-trivial topological phase and is in fact the

familiar Bernevig-Zhang-Hughes model [4] used to describe the quantum spin Hall effect in HgTe wells. We can see this by studying the eigenfunctions of $h(\mathbf{k})$:

$$\psi_{\pm}(\mathbf{k}) = \frac{1}{\sqrt{2d(d \pm d_3)}} \begin{pmatrix} d_3 \pm d \\ V(\sin k_x + i \sin k_y) \end{pmatrix} \tag{15}$$

where $d(\mathbf{k}) = \sqrt{d_3(\mathbf{k})^2 + V^2(\sin^2 k_x + \sin^2 k_y)}$, and $d_3(\mathbf{k}) = (\epsilon_c(\mathbf{k}) - \epsilon_f(\mathbf{k}))/2$. If $d_3(\mathbf{k}) > 0$ or $d_3(\mathbf{k}) < 0$ for all $\mathbf{k}$, these functions are well-defined on the entire BZ and the system is in a topologically trivial phase [34]. If this is not the case then it is impossible to choose a globally defined phase – the ground state wavefunction has nontrivial winding and characterizes a topological insulator. From Eq. 14, we see that this occurs when

$$-2 < \frac{\mu + \lambda + 2t_2}{t_1 - \chi} < 2\,. \tag{16}$$

Alternatively, we can obtain the same result by calculating the $\mathbb{Z}_2$ invariant ν [35]: when Eq. 16 holds, $\nu = -1$ and the system is a TI.

We will typically be studying systems with $|t_1| \gg |\chi|$ and $|t_2/t_1|$ small (implying μ and λ small as well), so Eq. 16 is not difficult to fulfill. In Fig. 1 the energy spectrum of the system in a slab geometry is shown for $J_H = 0.15$, $J_K = 0.3$. Half-filling is maintained on every site (see Appendix A), but V and χ were determined by self-consistently solving Eq. 9 in a periodic system. In Fig. 1(b), the topologically protected Dirac cone is clearly visible.

If we ignore the effect the boundary will have on the values of V, χ, and λ, we can calculate the Fermi velocity of the Dirac cone [34]:

$$v_F = 2V\sqrt{\frac{|\chi(t_1 - 2t_2)|}{|t_1 - 2t_2| + |\chi|}} \sim 2V\sqrt{|\chi|} \tag{17}$$

where we've assumed $|\chi| \ll t_1$ in the second equation. This is consistent with the prediction that the quasiparticles at the surface be heavy [8, 9, 26, 27]. For the parameters shown in Fig. 1, this formula predicts $v_F = 0.0592$, consistent with the numerically determined value $v_F = 0.0585$.

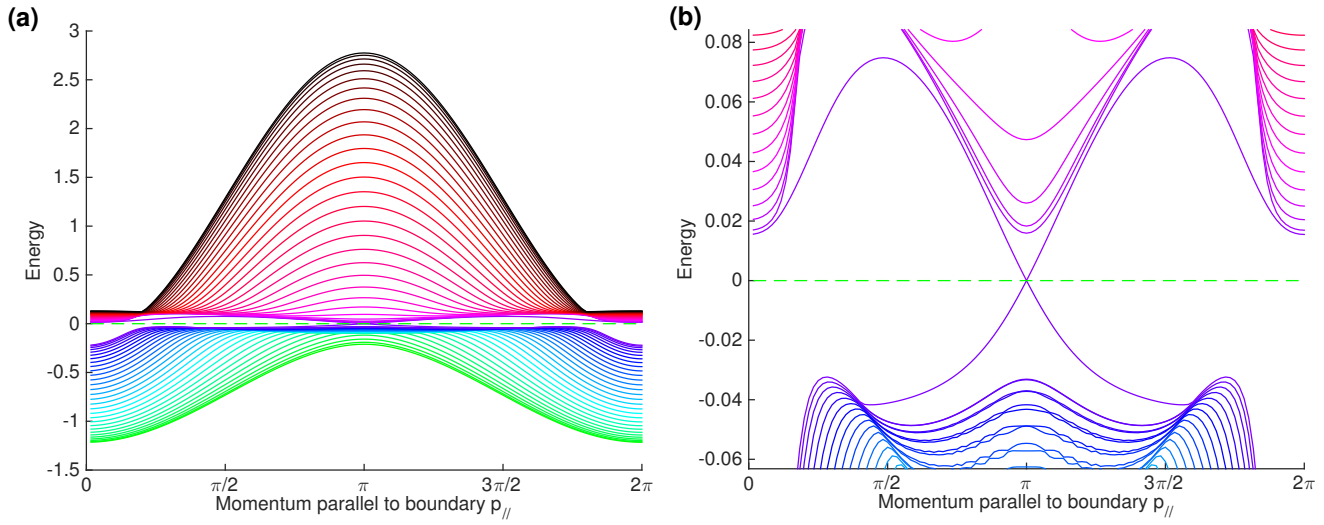

FIG. 1. (Color online) Energy spectrum for $J_H = 0.15$, $J_K = 0.3$. Both V and χ are constant throughout the bulk, but both μ_i and λ_i have been self-consistently solved to ensure that $n_c = n_f = 1$ on every site (see Appendix A). (a) The full spectrum is shown. (b) A closer view of the insulating gap, where the Dirac cone is clearly visible. We use units with $t_1 = 1.0$. Calculations were done with $t_2 = -0.25$ and at a temperature of 10^{-5}.

IV. SYSTEM WITH BOUNDARY

We now consider the effect the boundary will have on the mean field configuration and demonstrate the presence of two new fractionalized phases. Generally, we expect that the lower coordination number at the boundary will suppress the (nonlocal) hybridization: $V_{\text{surf}} \sim 3V_{\text{bulk}}/4$. While the decrease in V_{surf} will induce an increase in the spinon bond parameter $\chi_{i\mu}$ [36] both parallel and perpendicular to the surface, the parameter parallel to the surface will be more strongly affected. Since the Heisenberg coupling ultimately favors a non-uniform order [37], without a hybridization V to stabilize our mean field *ansatz* (Eq. 8), the anisotropy at the edge will result in a further decrease in the magnitude of the spinon bond parameter perpendicular to the surface, $|\chi_\perp|$. We always take a translationally invariant ansatz parallel to the surface, and so ignore the dimerization along the surface that arises in the large N limit of SU(N) antiferromagnets.

When these effects are predominant, an FL* on the surface is realized: the hybridization V_i vanishes on one or more layers at the surface and $\chi_\perp$ vanishes on the innermost layer. The existence of the SFL* phase is shown numerically by self-consistently solving Eqs. 9−11 in a slab geometry and comparing ground states energies (some details are given in Appendix A). The resulting phase diagram is shown in Fig. 2(a). In fact, we find two distinct SFL* phases: a decoupled spin chain

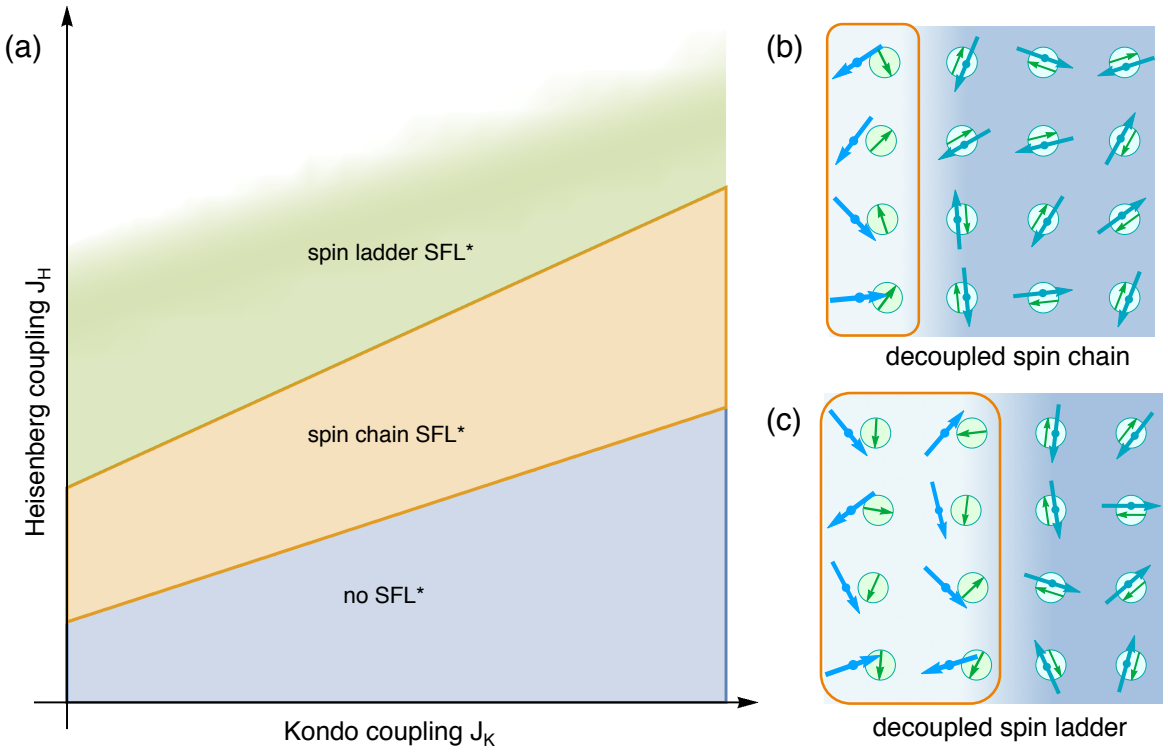

FIG. 2. (Color online) (a) Schematic phase diagram of surface states. (b),(c) Cartoon depictions of surface FL* states. In the dark blue region, the electron spins and localized moments are locked into singlets. Towards the edge (the pale blue region outlined in orange) the conduction electrons decouple from the moments, and the latter form a spin liquid. Naturally, the conduction electrons remain coupled to each other at all sites.

and a decoupled spin ladder, which are depicted in Figs. 2(b) and 2(c) respectively. In Fig. 3 we plot the spatial dependence of the mean field parameters in both SFL* states. The plots in the left column correspond to a spin chain SFL* state whereas the right column corresponds to a spin ladder SLF* state. The phases are distinguished by whether V vanishes on the first site only or on both the first and second site, shown in Fig. 3(a) and (b) respectively. In Figs. 3(c) and (d) our intuition regarding the behaviour of χ near the boundary is confirmed: $|\chi_\perp|$ is suppressed to zero whereas $|\chi_\parallel|$ increases to the value it would assume in a single dimension. The fluctuations of the Lagrange multiplier field λ (Figs. 3(e) and (f)) are a reflection of the on-site requirement of half-filling for both the spinons and electons.

In Fig. 4(a), the spectrum of the spin chain SFL* state is shown. The red dash-dotted curve is the dispersion of the spinons calculated at mean field. While we do not claim that this accurately represents the Heisenberg chain, we nonetheless expect gapless spin excitations [38]. The remaining in-gap states can be understood as the result of the mixing of the surface layer of conduction

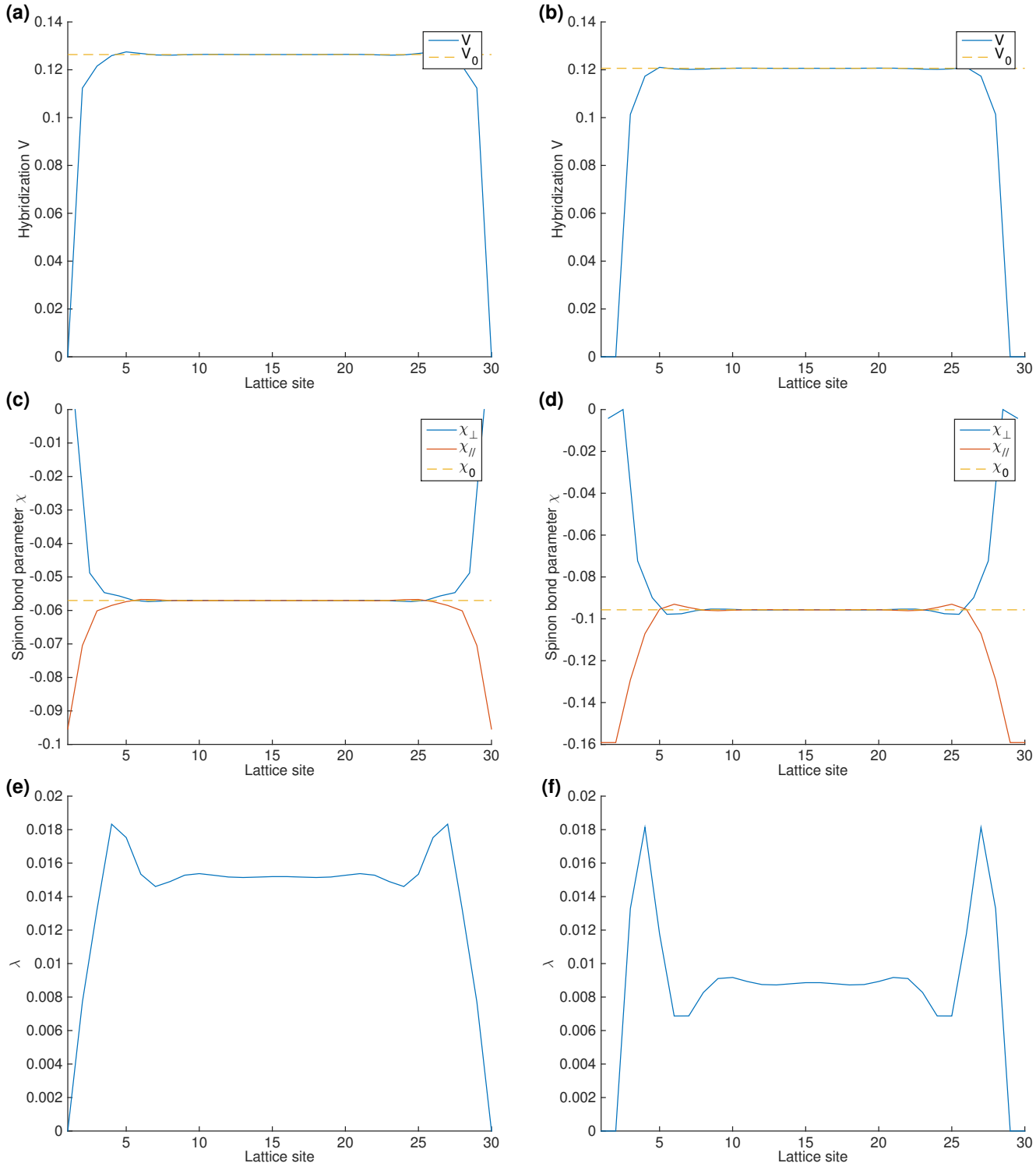

FIG. 3. (Color online) Spatial dependence of mean field parameters in SFL* phases. In the left column, we plot values corresponding to the spin chain SFL* ($J_H = 0.15$, $J_K = 0.3$) while on the right values corresponding to the spin ladder SFL* ($J_H = 0.25$, $J_K = 0.3$) are shown. (a),(b) Hybridization V_i. (c),(d) Spinon bond parameters $\chi_{i\mu}$ in the direction perpendicular (blue) and parallel (red) to the boundary. (e),(f) The Lagrange multiplier field λ_i. In (a)−(f), the yellow dashed line plots the value obtained in the translationally invariant case. We use units with $t_1 = 1.0$. Calculations were done with $t_2 = -0.25$ and at a temperature of 10^{-5}.

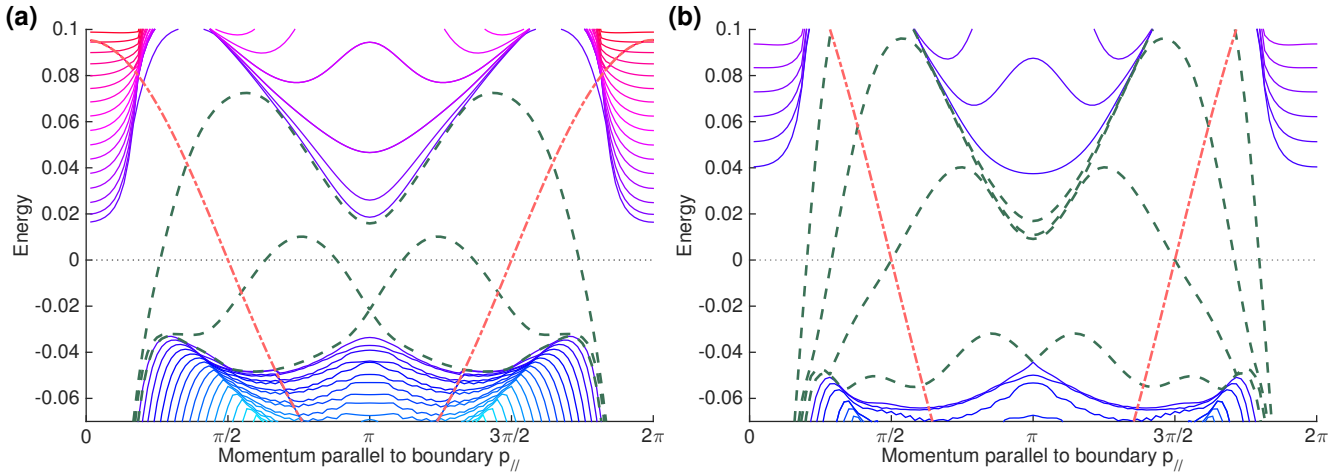

FIG. 4. (Color online) Energy spectra in SFL* phases. The green dashed curves show the dispersion of the (primarily) electronic surface states while the dash-dotted red curve represents the one-dimensional cosine dispersion found for the spinons and is merely an artifact of the *ansatz*. All other colours correspond to bulk states. (a) Spin chain SFL* ($J_H = 0.15$, $J_K = 0.3$). The ground state has $V_i = 0$ on the first surface layer and the moments form a spin chain decoupled from the bulk. (b) Spin ladder SFL* ($J_H = 0.25$, $J_K = 0.3$). The ground state has $V_i = 0$ on the first two layers and a spin ladder whose spectrum is beyond the field of view is present on the surface. We use units with $t_1 = 1.0$. Calculations were done with $t_2 = -0.25$ and at a temperature of 10^{-5}.

electron with the Dirac cone. Consistent with its topology, even if the Dirac cone is no longer present at the chemical potential, two chiral bands traverse the gap from the conduction to the valence band and the surface is metallic. In this case, an additional four metallic surface states per spin are present, but these are not topologically protected and we can imagine pushing them below the chemical potential in a number of ways, such as, for instance, softening the restriction imposed by Eq. 11.

The spectrum corresponding to the second surface FL* state, the decoupled spin ladder, is shown in Fig. 4(b). As necessary, the lowest energy configuration of the spinon is gapped [38, 39], with $\chi_{\parallel} = 0$ and $\chi_{\perp} = -J_H$ on the surface.. Their contribution to the spectrum is outside of the field of view in Fig. 4(b).

In both phases, the metallic bands have lighter quasiparticles than predicted by the translationally invariant theory in Eq. 17. For the spin chain, the surface velocity of the leftmost state in Fig. 4(a) is $v_F = 0.095$, compared to $v_F = 0.052$ for the Dirac cone of Fig. 1(b). For the spin ladder, the effect is even more pronounced. There, the lightest state has a Fermi velocity of $v_F = 0.48$ compared to the translationally-invariant value $v_F = 0.072$.

We do not expect our model to realize any further SFL* phases; the coordination number

effects which stabilize the spin chain and ladder phases become negligible when the number of decoupled layers increases. In fact, when J_H becomes very large, the mean field calculations become unreliable. When it is no longer energetically favourable for the electrons and spins to hybridize, our mean field *ansatz* ceases to be a valid description and a more complicated mean field theory which allows for magnetic order is required. While the vanishing of V does not pose the same numerical problem for the SFL* states discussed here, the gapless spectrum determined for the spin ladder state is a manifestation of this issue.

The structure of the fractionalized excitations in the SFL* states found here is rather simple: just a free gas of neutral $S = 1/2$ spinon excitations. We view this mainly as a 'proof of principle' that such SFL* states can exist on the surface of TKI. Clearly, more complex types of spin liquid states, or states with valence bond solid order are possible on the surface; for three-dimensional TKI with two-dimensional surfaces, magnetic order is also possible on the surface. Clearly, the stability of a spin liquid phase against these other orders is dependent upon the presence of frustrating interactions, but this difficult issues cannot be addressed by our simplified mean-field theory.

V. DISCUSSION

The strong electron-electron interactions in topological Kondo insulators make them appealing candidates for searching for novel correlated electron states. In many heavy-fermion compounds, the strong interactions acting on the f-electron local moments are quenched by the Kondo screening of the conductions electrons, and the resulting state is eventually a Fermi liquid, or a band insulator for suitable density. The topological Kondo insulators offer the attractive possibility that the hybridization between the local moments and the conduction electron states can be weakened near the surface [22, 24], and this could explain the light effective masses associated with the surface electronic states [17–19]. With the weakened hybridization, we have proposed here that the local moments may form a spin liquid state with 'intrinsic' topological order. As the fractionalized excitations of such a spin liquid co-exist with the conduction electron surface states similar to those of a conventional TI, the surface realizes a fractionalized Fermi liquid [29, 30].

This paper has presented mean-field solutions of Kondo-Heisenberg model on a square lattice which act as a proof-of-principle of the enhanced stability of the such surface fractionalized Fermi liquids (SFL*). We fully expect that such solutions also exist on the surfaces of three-dimensional

lattices, relevant to a Kondo insulator like SmB_6.

Experimental verification of this phase in a physical system could be achieved by comparing the number of charge carriers to the number of gapless degrees of freedom at the surface. For instance, both the electrons and the spinons will contribute to the thermal conductivity and spin susceptibility; conversely, transport and quantum oscillation measurements can only detect the charge carriers. Since the bulk is gapped, a discrepancy between these two types of measurements would indicate the realization of an SFL*.

The recent evidence for *bulk* quantum oscillations in insulating SmB_6 [40] is exciting evidence for the non-trivial many-electron nature of these materials. It has been proposed [41] that these oscillations appear because the magnetic field effects are stronger than the weak hybridization between the conduction electrons and the local moments. In a more self-consistent analysis we can envisage that the hybridization vanishes for strong-enough magnetic fields, and this releases the conduction electrons to form Fermi surfaces leading to the quantum oscillations. Then the local moments transverse to the applied field will form a bulk spin liquid, controlled by the larger J_H coupling, similar to the surface spin liquid we have discussed here. Thus, while we have proposed here the formation of a SLF* states in SmB_6 in zero magnetic field, it may well be that a bulk FL* state forms in high magnetic field. Establishing the existence of the bulk FL* would require confirming that the quantum oscillations are from the bulk, and ensuring that the field has not induced any antiferromagnetic or density wave order: then the violation of the Luttinger total Fermi volume in the quantum oscillation implies the existence of topological order [30], and the FL* is the simplest candidate.

ACKNOWLEDGMENTS

We thank D. Chowdhury for significant discussions at the early stages of this project. We also thank S. Sebastian and J. D. Sau for helpful discussion. AT is supported by NSERC. This research was supported by the NSF under Grant DMR-1360789. Research at Perimeter Institute is supported by the Government of Canada through Industry Canada and by the Province of Ontario through the Ministry of Research and Innovation.

Appendix A: Mean field theory with boundary

In this appendix, we consider the mean field equations in the presence of a boundary. We define the lattice to be finite in the x-direction, $x_i = 1, \ldots, N$, and infinite in the y-direction (to remove factors of i, we actually switch the x- and y-directions compared to Eq. 5). We rewrite the Fourier transform, which is now only valid in the y-direction:

$$\begin{aligned} c_{ij\sigma} &= \int \frac{dk}{2\pi} e^{iky_j} c_{ik\sigma}, \qquad & d_{ij\alpha} &= \int \frac{dk}{2\pi} e^{iky_j} \left[2\alpha \sin k \, c_{ik\alpha} + (c_{j+1,k\alpha} - c_{i-1,k\alpha})\right], \\ f_{ij\sigma} &= \int \frac{dk}{2\pi} e^{iky_j} f_{ik\sigma}. \end{aligned} \tag{A1}$$

Translational invariance in the y-direction implies that the mean field parameters will depend only on the distance from the boundary – the roman indices i, j, etc. label the x-coordinate only. We express the Hamiltonian in block form as

$$\begin{aligned} \hat{H}_{MF} &= \sum_k \Psi^\dagger_{k\sigma} \mathcal{H}_\sigma(k) \Psi_{k\sigma}, \qquad & \Psi^\dagger_{k\sigma} &= \left(c^\dagger_{1k\sigma}, c^\dagger_{2k\sigma}, \ldots, f^\dagger_{1k\sigma}, f^\dagger_{2k\sigma}, \ldots\right) \\ & & &= \left(\psi^\dagger_{1k\sigma}, \psi^\dagger_{2k\sigma}, \ldots, \psi^\dagger_{1+N,k\sigma}, \psi^\dagger_{2+N,k\sigma}, \ldots\right) \\ \mathcal{H}_\uparrow(k) &= \begin{pmatrix} h_c(k) & h_{cf}(k) \\ h^\dagger_{cf}(k) & h_f(k) \end{pmatrix} \qquad & \mathcal{H}_\downarrow(k) &= \mathcal{H}_\uparrow(-k)^* \end{aligned} \tag{A2}$$

with blocks given by

$$h_c(k) = -\frac{t_1}{2} \begin{pmatrix} 2\cos k & 1 & 0 & \cdots \\ 1 & 2\cos k & 1 & \cdots \\ 0 & 1 & 2\cos k & \cdots \\ \vdots & \vdots & \vdots & \ddots \end{pmatrix} - t_2 \cos k \begin{pmatrix} 0 & 1 & 0 & \cdots \\ 1 & 0 & 1 & \cdots \\ 0 & 1 & 0 & \cdots \\ \vdots & \vdots & \vdots & \ddots \end{pmatrix} - \begin{pmatrix} \mu_1 & 0 & 0 & \cdots \\ 0 & \mu_2 & 0 & \cdots \\ 0 & 0 & \mu_3 & \cdots \\ \vdots & \vdots & \vdots & \ddots \end{pmatrix} \tag{A3}$$

$$h_f(k) = -\frac{1}{2}\begin{pmatrix} 2\chi_{1y}\cos k & \chi_{1x} & 0 & 0 & \cdots & \cdots & \cdots \\ \chi_{1x} & 2\chi_{2y}\cos k & \chi_{2x} & 0 & \cdots & \cdots & \cdots \\ 0 & \chi_{2x} & 2\chi_{3y}\cos k & \chi_{3x} & \cdots & \cdots & \cdots \\ \vdots & \vdots & \vdots & \vdots & \ddots & \cdots & \cdots \\ \vdots & \vdots & \vdots & \vdots & \vdots & 2\chi_{N-1,y}\cos k & \chi_{N-1,x} \\ \vdots & \vdots & \vdots & \vdots & \vdots & \chi_{N-1,x} & 2\chi_{Ny}\cos k \end{pmatrix} + \begin{pmatrix} \lambda_1 & 0 & 0 & 0 & \cdots & \cdots & \cdots \\ 0 & \lambda_2 & 0 & 0 & \cdots & \cdots & \cdots \\ 0 & 0 & \lambda_3 & 0 & \cdots & \cdots & \cdots \\ \vdots & \vdots & \vdots & \vdots & \ddots & \cdots & \cdots \\ \vdots & \vdots & \vdots & \vdots & \vdots & \lambda_{N-1} & 0 \\ \vdots & \vdots & \vdots & \vdots & \vdots & 0 & \lambda_N \end{pmatrix} \tag{A4}$$

$$h_{cf}(k) = \frac{1}{2}\begin{pmatrix} 2V_1\sin k & -V_2 & 0 & \cdots \\ V_1 & 2V_2\sin k & -V_3 & \cdots \\ 0 & V_2 & 2V_3\sin k & \cdots \\ \vdots & \vdots & \vdots & \ddots \end{pmatrix}. \tag{A5}$$

To determine correlation functions, we diagonalize the Hamiltonian numerically. For each k, we find the matrices $U(k)$ such that

$$U^\dagger \mathcal{H}(k) U(k) = \Lambda(k), \qquad \Lambda_{ij}(k) = \delta_{ij} E_j(k)\,. \tag{A6}$$

Then, the mean field equations of Eqs. $9-11$ may be expressed as

$$1 = \sum_\alpha \int \frac{dk}{2\pi} \left\langle f^\dagger_{kj\alpha} f_{kj\alpha} \right\rangle = \sum_\alpha \int \frac{dk}{2\pi} \left\langle \psi^\dagger_{k,j+N,\alpha} \psi_{k,j+N,\alpha} \right\rangle = 2\int \frac{dk}{2\pi} \sum_{l=1}^{2N} n(E_l(k)) U_{j+N,l}(k) U^\dagger_{l,j+N}(k) \tag{A7}$$

$$1 = \sum_\alpha \int \frac{dk}{2\pi} \left\langle c^\dagger_{kj\alpha} c_{kj\alpha} \right\rangle = \sum_\alpha \int \frac{dk}{2\pi} \left\langle \psi^\dagger_{kj\alpha} \psi_{kj\alpha} \right\rangle = 2\int \frac{dk}{2\pi} \sum_{l=1}^{2N} n(E_l(k)) U_{jl}(k) U^\dagger_{lj}(k) \tag{A8}$$

$$
\begin{aligned}
V_i &= -\frac{J_K}{2}\sum_\alpha \int \frac{dk}{2\pi}\left\langle d^\dagger_{ik\alpha} f_{ik\alpha}\right\rangle = -\frac{J_K}{2}\sum_\alpha \int \frac{dk}{2\pi}\left[2\alpha \sin k \left\langle c^\dagger_{ik\alpha} f_{ik\alpha}\right\rangle + \left\langle c^\dagger_{i+1,k\alpha} f_{ik\alpha}\right\rangle - \left\langle c^\dagger_{i-1,k\alpha} f_{ik\alpha}\right\rangle\right] \\
&= -\frac{J_K}{2}\sum_\alpha \int \frac{dk}{2\pi}\left[2\alpha \sin k \left\langle \psi^\dagger_{ik\alpha} \psi_{i+N,k\alpha}\right\rangle + \left\langle \psi^\dagger_{i+1,k\alpha} \psi_{i+N,k\alpha}\right\rangle - \left\langle \psi^\dagger_{i-1,k\alpha} \psi_{i+N,k\alpha}\right\rangle\right] \\
&= -J_K \int \frac{dk}{2\pi}\sum_{l=1}^{2N} n(E_l(k))\left[2\sin k\, U_{i+N,l}(k) U^\dagger_{l,i}(k) + U_{i+N,l}(k) U^\dagger_{l,i+1}(k) - U_{i+N,l}(k) U^\dagger_{l,i-1}(k)\right]
\end{aligned} \tag{A9}
$$

$$
\begin{aligned}
\chi_{ix} &= \frac{J_H}{2}\sum_\alpha \int \frac{dk}{2\pi}\left[\left\langle f^\dagger_{i+1,k\alpha} f_{ik}\right\rangle + \left\langle f^\dagger_{ik\alpha} f_{i+1,k\alpha}\right\rangle\right] \\
&= \frac{J_H}{2}\sum_\alpha \int \frac{dk}{2\pi}\left[\left\langle \psi^\dagger_{i+N+1,k\alpha} \psi_{i+N,k\alpha}\right\rangle + \left\langle \psi^\dagger_{i+N,k\alpha} \psi_{i+N+1,k\alpha}\right\rangle\right] \\
&= J_H \int \frac{dk}{2\pi}\sum_{l=1}^{2N} n(E_l(k))\left[U_{i+N,l}(k) U^\dagger_{l,i+N+1}(k) + U_{i+N,1,l}(k) U^\dagger_{l,i+N+1}(k)\right]
\end{aligned} \tag{A10}
$$

$$
\begin{aligned}
\chi_{iy} &= \frac{J_H}{2}\sum_\alpha \int \frac{dk}{2\pi} 2\cos k \left\langle f^\dagger_{ik\alpha} f_{ik\alpha}\right\rangle = J_H \sum_\alpha \int \frac{dk}{2\pi}\cos k \left\langle \psi^\dagger_{i+N,k\alpha} \psi_{i+N,k\alpha}\right\rangle \\
&= 2\, J_H \int \frac{dk}{2\pi}\sum_{l=1}^{2N} n(E_l(k)) \cos k\, U_{i+N,l}(k) U^\dagger_{l,i+N}(k)
\end{aligned} \tag{A11}
$$

[1] M. Z. Hasan and C. L. Kane, "*Colloquium*: Topological insulators," Rev. Mod. Phys. **82**, 3045 (2010).

[2] X.-L. Qi and S.-C. Zhang, "Topological insulators and superconductors," Rev. Mod. Phys. **83**, 1057 (2011).

[3] C. L. Kane and E. J. Mele, "Z_2 Topological Order and the Quantum Spin Hall Effect," Phys. Rev. Lett. **95**, 146802 (2005).

[4] B. A. Bernevig, T. L. Hughes, and S.-C. Zhang, "Quantum Spin Hall Effect and Topological Phase Transition in HgTe Quantum Wells," Science **314**, 1757 (2006).

[5] J. E. Moore and L. Balents, "Topological invariants of time-reversal-invariant band structures," Phys. Rev. B **75**, 121306 (2007).

[6] L. Fu, C. L. Kane, and E. J. Mele, "Topological insulators in three dimensions," Phys. Rev. Lett. **98**, 106803 (2007).

[7] R. Roy, "Z_2 classification of quantum spin hall systems: An approach using time-reversal invariance," Phys. Rev. B **79**, 195321 (2009).

[8] M. Dzero, K. Sun, V. Galitski, and P. Coleman, "Topological Kondo Insulators," Phys. Rev. Lett. **104**, 106408 (2010).

[9] M. Dzero, K. Sun, P. Coleman, and V. Galitski, "Theory of topological Kondo insulators," Phys. Rev. B **85**, 045130 (2012).

[10] M. Dzero, J. Xia, V. Galitski, and P. Coleman, "Topological Kondo Insulators," Annual Review of Condensed Matter Physics, to appear (2015), arXiv:1506.05635 [cond-mat.str-el].

[11] S. Doniach, "The Kondo lattice and weak antiferromagnetism," Physica B+C **91**, 231 (1977).

[12] S. Wolgast, C. Kurdak, K. Sun, J. W. Allen, D.-J. Kim, and Z. Fisk, "Low-temperature surface conduction in the Kondo insulator SmB_6," Phys. Rev. B **88**, 180405 (2013).

[13] D. J. Kim, T. Grant, and Z. Fisk, "Limit Cycle and Anomalous Capacitance in the Kondo Insulator SmB_6," Phys. Rev. Lett. **109**, 096601 (2012).

[14] X. Zhang, N. P. Butch, P. Syers, S. Ziemak, R. L. Greene, and J. Paglione, "Hybridization, Inter-Ion Correlation, and Surface States in the Kondo Insulator SmB_6," Phys. Rev. X **3**, 011011 (2013).

[15] W. A. Phelan, S. M. Koohpayeh, P. Cottingham, J. W. Freeland, J. C. Leiner, C. L. Broholm, and T. M. McQueen, "Correlation between Bulk Thermodynamic Measurements and the Low-Temperature-Resistance Plateau in SmB_6," Phys. Rev. X **4**, 031012 (2014).

[16] D. J. Kim, S. Thomas, T. Grant, J. Botimer, Z. Fisk, and J. Xia, "Surface Hall effect and nonlocal transport in SmB_6: evidence for surface conduction," Scientific reports **3** (2013).

[17] M. Neupane, N. Alidoust, S.-Y. Xu, T. Kondo, Y. Ishida, D. J. Kim, C. Liu, I. Belopolski, Y. J. Jo, T.-R. Chang, H.-T. Jeng, T. Durakiewicz, L. Balicas, H. Lin, A. Bansil, S. Shin, Z. Fisk, and M. Z. Hasan, "Surface electronic structure of the topological Kondo-insulator candidate correlated electron system SmB_6," Nat Commun **4** (2013).

[18] J. Jiang, S. Li, T. Zhang, Z. Sun, F. Chen, Z. R. Ye, M. Xu, Q. Q. Ge, S. Y. Tan, X. H. Niu, M. Xia, B. P. Xie, Y. F. Li, X. H. Chen, H. H. Wen, and D. L. Feng, "Observation of possible topological in-gap surface states in the Kondo insulator SmB_6 by photoemission," Nat Commun **4** (2013).

[19] N. Xu, X. Shi, P. K. Biswas, C. E. Matt, R. S. Dhaka, Y. Huang, N. C. Plumb, M. Radović, J. H. Dil, E. Pomjakushina, K. Conder, A. Amato, Z. Salman, D. M. Paul, J. Mesot, H. Ding, and M. Shi, "Surface and bulk electronic structure of the strongly correlated system SmB_6 and implications for

a topological Kondo insulator," Phys. Rev. B **88**, 121102 (2013).

[20] J. D. Denlinger, J. W. Allen, J.-S. Kang, K. Sun, B.-I. Min, D.-J. Kim, and Z. Fisk, "SmB_6 Photoemmission: Past and Present," JPS Conf. Proc. **3**, 017038 (2014).

[21] J. Jiang, S. Li, T. Zhang, Z. Sun, F. Chen, Z. R. Ye, M. Xu, Q. Q. Ge, S. Y. Tan, X. H. Niu, M. Xia, B. P. Xie, Y. F. Li, X. H. Chen, H. H. Wen, and D. L. Feng, "Observation of possible topological in-gap surface states in the Kondo insulator SmB_6 by photoemission," Nat Commun **4** (2013).

[22] B. Roy, J. D. Sau, M. Dzero, and V. Galitski, "Surface theory of a family of topological Kondo insulators," Phys. Rev. B **90**, 155314 (2014).

[23] P. Nikolić, "Two-dimensional heavy fermions on the strongly correlated boundaries of Kondo topological insulators," Phys. Rev. B **90**, 235107 (2014).

[24] V. Alexandrov, P. Coleman, and O. Erten, "Kondo Breakdown in Topological Kondo Insulators," Phys. Rev. Lett. **114**, 177202 (2015).

[25] J. Iaconis and L. Balents, "Many-body effects in topological Kondo insulators," Phys. Rev. B **91**, 245127 (2015).

[26] V. Alexandrov, M. Dzero, and P. Coleman, "Cubic Topological Kondo Insulators," Phys. Rev. Lett. **111**, 226403 (2013).

[27] F. Lu, J. Zhao, H. Weng, Z. Fang, and X. Dai, "Correlated Topological Insulators with Mixed Valence," Phys. Rev. Lett. **110**, 096401 (2013).

[28] L. Balents, "Spin liquids in frustrated magnets," Nature **464**, 199 (2010).

[29] T. Senthil, S. Sachdev, and M. Vojta, "Fractionalized Fermi Liquids," Phys. Rev. Lett. **90**, 216403 (2003).

[30] T. Senthil, M. Vojta, and S. Sachdev, "Weak magnetism and non-Fermi liquids near heavy-fermion critical points," Phys. Rev. B **69**, 035111 (2004).

[31] B. Coqblin and J. R. Schrieffer, "Exchange interaction in alloys with cerium impurities," Phys. Rev. **185**, 847 (1969).

[32] P. W. Anderson, "Localized Magnetic States in Metals," Phys. Rev. **124**, 41 (1961).

[33] J. R. Schrieffer and P. A. Wolff, "Relation between the Anderson and Kondo Hamiltonians," Phys. Rev. **149**, 491 (1966).

[34] B. A. Bernevig and T. L. Hughes, *Topological Insulators and Topological Superconductors* (Princeton University Press, 2013).

[35] L. Fu and C. L. Kane, "Topological insulators with inversion symmetry," Phys. Rev. B **76**, 045302 (2007).

[36] I. Paul, C. Pépin, and M. R. Norman, "Multiscale fluctuations near a Kondo breakdown quantum critical point," Phys. Rev. B **78**, 035109 (2008).

[37] N. Read and S. Sachdev, "Some features of the phase diagram of the square lattice SU(N) antiferromagnet," Nuclear Physics B **316**, 609 (1989).

[38] F. D. M. Haldane, "O(3) nonlinear σ model and the topological distinction between integer- and half-integer-spin antiferromagnets in two dimensions," Phys. Rev. Lett. **61**, 1029 (1988).

[39] T. Giamarchi, *Quantum Physics in One Dimension*, International Series of Monographs on Physics (Clarendon Press, 2003).

[40] B. S. Tan, Y.-T. Hsu, B. Zeng, M. C. Hatnean, N. Harrison, Z. Zhu, M. Hartstein, M. Kiourlappou, A. Srivastava, M. D. Johannes, T. P. Murphy, J.-H. Park, L. Balicas, G. G. Lonzarich, G. Balakrishnan, and S. E. Sebastian, "Unconventional Fermi surface in an insulating state," Science **349**, 287 (2015).

[41] J. Knolle and N. R. Cooper, "Quantum Oscillations without a Fermi Surface and the Anomalous de Haas-van Alphen Effect," Phys. Rev. Lett. **115**, 146401 (2015).